Structure and Reactivity of Halogenated GC PNA Base Pairs – A DFT Approach

Ranjithkumar Rajamani[1], Indumathi K[2], Srimathi P[2], Praveena G[2*],
Ling Shing Wong[3], Sinouvassane Djearamane[4,5*]

[1]Viyen Biotech LLP, Coimbatore, Tamil Nadu 641031, India
[2]Department of Physics, PSGR Krishnammal College for Women, Coimbatore, Tamilnadu, 641004, India
[3]Life Science Division, Faculty of Health and Life Sciences, INTI International University, Nilai, 71800, Malaysia
[4]Department of Biomedical Science, Faculty of Science, UniversitiTunku Abdul Rahman, Kampar 31900, Perak, Malaysia
[5]Biomedical Research Unit and Lab Animal Research Centre, Saveetha Dental College, Saveetha Institute of Medical and Technical Sciences, Saveetha University, Chennai 602 105, India

ABSTRACT

The present study explored the structural and reactivity relationship of halogenated G-C PNA base pairs using density functional theory (DFT) calculations. The halogens such as F, Cl, and Br are substituted by replacing H atoms involved in H-bonds of the base pairs. All structures were optimized using the B3LYP/6-311++G** theory level, and positive frequencies confirmed their equilibrium states. To understand the structural variations of the considered halogenated systems, the bond distances of R─X, R─H, and X/H•••Y and the bond angles of R─X•••Y were analyzed. The obtained structural parameters and interaction energies are comparable with the previous theoretical reports. In addition, the interaction energies (E_{int}) and quantum molecular descriptors (QMD) are also calculated to understand the difference between halogenated PNA systems and their non-halogenated counterparts. In this study, the enhancement in the reactivity properties ω, χ, EA and S of halogenated PNA systems has been demonstrated, which indicates their improved responsive characteristics in various chemical reactions. Based on the available results, the halogenated PNA systems, carefully considering their substitutional position, facilitate better accommodation for the triplex formation of dsDNA/dsRNA. Therefore, it is concluded that the improved reactivity properties of halogenated PNA base pairs would make them potential candidates for various biological applications.

* Corresponding author

E-mail: praveenag@psgrkcw.ac.in (Praveena G);
          sinouvassane@utar.edu.my (Sinouvassane Djearamane)

1 Introduction

Promoting the formation of halogen bonds in biomolecules is an effective method for engineering new artificial proteins and nucleotides (Metrangolo and Resnati 2008). In biomolecules, a halogen bond can be generally defined as R—X•••Y—R′, where "X" represents a halogen atom in one molecule (R—X) and "Y" represents an electron-rich group (Y—R′) such as oxygen, nitrogen, and so on (Auffinger et al. 2004). Especially in nucleic acid systems, for example, halogens can strengthen the base stacking interaction, paving the way for enhancing the stability of higher-ordered strands (Kolář and Tabarrini 2017). Furthermore, Auffinger et al. (2004) have demonstrated the effectiveness of a brominated DNA complex d(CCAGTACbr^5UGG) (br^5U, 5-bromouridine) in ligand binding, molecular recognition events, and molecular folding. The molecular-level insights of halogenated Watson-Crick base pairs have been studied by Parker et al. (2012) and Gomila et al. (2023) using theoretical techniques. They found that brominated structures form more stable complexes due to their size and polarizability. Several halogenated drugs, containing either fluorine or chlorine, or both, have been used commercially to treat various diseases, including migraine, various cancer types, cardiovascular disease, vasculitis and multiple sclerosis. These drugs were sanctioned by the Food and Drug Administration (FDA) (Inoue et al. 2020; Yu et al. 2021). For example, vancomycin, a chlorine-containing antibiotic drug, is used to treat MRSA infections (Álvarez-Martínez et al. 2020). Recently, anticancer halogenated medicines such as tivozanib, melphalan flufenamide, sotorasib, asciminib, umbralisib and infringatinib were approved in 2021 to limit the growth of cancer cells by controlling various kinds of biological activities (Benedetto Tiz et al. 2022).

Moreover, studies have shown that the incorporation of 5-bromocytosine, 5-halo-2′-deoxyuridines bromodeoxyuridine and iododeoxyuridine as nucleoside into the cellular DNA can potentially act as a photosensitizer to detect the breakages and cross-links in DNA strands (Wang and Lu 2010; Zdrowowicz et al. 2016). Chemically modified nucleic acid structures have received notable attention in scientific investigation since their usage has been found in in vivo applications (Ochoa and Milam 2020). In this approach, Peptide nucleic acid (PNA), an artificial oligonucleotide, was modeled by Nielsen et al. (1992) and found interesting biological applications since it is the best compensation for phosphate backbone in DNA. The same group examined the rival biostability of the PNA H-T10-LysNH2 against proteases using various bodily fluids such as cellular extracts in human serum and bacterial and ascites tumour cell extracts (Demidov et al. 1994). Patil et al. (2018) formed the triplex strand by using double-stranded RNA (dsRNA) with single-stranded PNA (ssPNA), wherein the utilization of halouracil complexes showed a significant impact on strengthening the adjacent

bases via H-bond interactions, enhancing well-ordered triplex strands. On the other hand, studies revealed that the incorporation of halogens into the peptide/protein complexes is capable of conformational stabilization due to the directionality and strength compared to that of an analogous H-bond, proving their implementation in protein engineering (Danelius et al. 2017). Considering the influential role of halo-modified nucleic acid constituents for various biological purposes, we systematically designed a peptidic chain linked 9 halogenated GC base pairs, named $G_{PNA}C_{PNA}$-F^1, $G_{PNA}C_{PNA}$-F^2, $G_{PNA}C_{PNA}$-F^3, $G_{PNA}C_{PNA}$-Cl^1, $G_{PNA}C_{PNA}$-Cl^2, $G_{PNA}C_{PNA}$-Cl^3, $G_{PNA}C_{PNA}$-Br^1, $G_{PNA}C_{PNA}$-Br^2 and $G_{PNA}C_{PNA}$-Br^3 to explore their structure and reactivity relationship properties applying quantum chemical techniques. Thus, the main purpose of this study is to focus on revealing the structure and reactivity properties of halogenated PNA base pairs, emphasizing their substitutional positions.

2 Materials and Methods

2.1 System setup and computational methods

Halogenated PNA base-pair structures were systematically designed by the substitution of halogens (X=F, Cl, and Br, where s in X^s represent the position of the halogen atom in H-bonds, as numbered in Figure 1) at each possible site of the H-bond. In contrast, the peptide linkage N-(2-aminoethyl)-glycine is connected via the N^{9th} position of Guanine and the N^{1st} position of Cytosine. Totally, 9 halogenated GC PNA base pair structures such as $G_{PNA}C_{PNA}$-F^1, $G_{PNA}C_{PNA}$-F^2, $G_{PNA}C_{PNA}$-F^3, $G_{PNA}C_{PNA}$-Cl^1, $G_{PNA}C_{PNA}$-Cl^2, $G_{PNA}C_{PNA}$-Cl^3, $G_{PNA}C_{PNA}$-Br^1, $G_{PNA}C_{PNA}$-Br^2 and $G_{PNA}C_{PNA}$-Br^3 were obtained (Figure 1). As Density functional theory (DFT) being extensively used to study the H-bonded systems and organic molecules (Fonseca Guerra et al. 2000) for providing reliable results, we have chosen B3LYP functional (Lee et al. 1988) for the present work to study the structure and reactivity relationship of halogenated PNA systems. All considered structures were constructed using Chemcraft software (https://www.chemcraftprog.com) and are optimized at B3LYP/6-311++G** level of theory with the help of the Gaussian 09W program suite (Gaussian 09, A Revision 2016). Positive frequencies confirmed the equilibrium state of the ground state structures. The following analyses were conducted to examine the structure and reactivity of halogenated PNA base pairs: structural parameters, interaction energies (E_{int}) and quantum molecular descriptors (QMD). In addition, molecular electrostatic potential (MESP) was generated for the optimized structures using the Gaussview 5.0 package (Dennington et al. 2009). The plots of MESP were generated in atomic units (Hartrees), and an isodensity surface value was fixed at 0.004 electrons/bohr^3 for all the systems studied (Figure 2). The theoretical description of the present work is provided below.

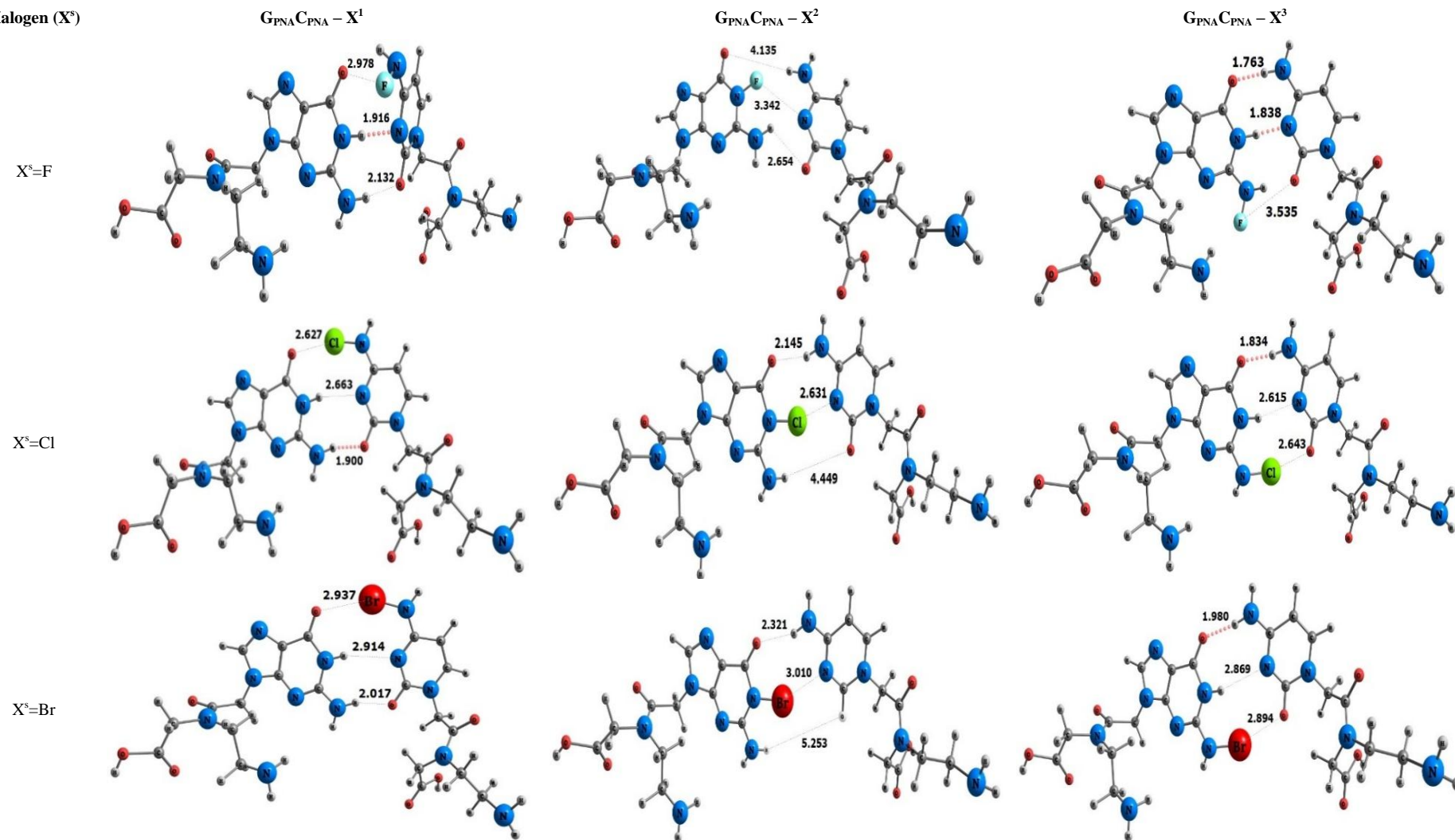| Halogen (X^s)	$G_{PNA}C_{PNA} - X^1$	$G_{PNA}C_{PNA} - X^2$	$G_{PNA}C_{PNA} - X^3$

Figure 1 Optimized structures of $G_{PNA}C_{PNA}$-F^1, $G_{PNA}C_{PNA}$-F^2, $G_{PNA}C_{PNA}$-F^3, $G_{PNA}C_{PNA}$-Cl^1, $G_{PNA}C_{PNA}$-Cl^2, $G_{PNA}C_{PNA}$-Cl^3, $G_{PNA}C_{PNA}$-Br^1, $G_{PNA}C_{PNA}$-Br^2 and $G_{PNA}C_{PNA}$-Br^3 obtained at B3LYP/6-311++G** level of theory.

| Halogen (X^s) | G$_{PNA}$C$_{PNA}$ – X^1 | G$_{PNA}$C$_{PNA}$ – X^2 | G$_{PNA}$C$_{PNA}$ – X^3 |

-7.476e-2   7.476e-2

X^s=F

X^s=Cl

X^s=Br
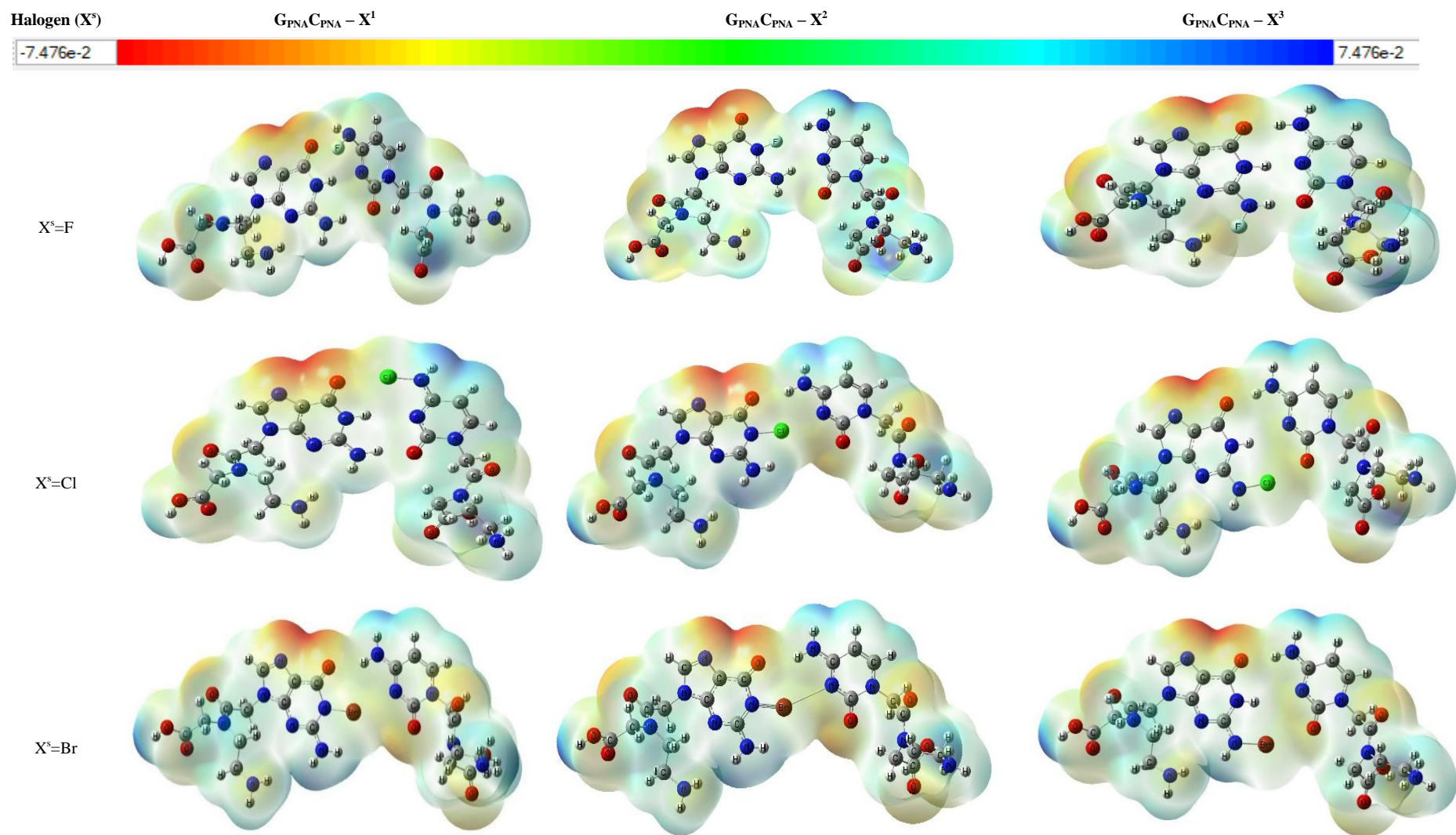
Figure 2 Electrostatic potential maps of G$_{PNA}$C$_{PNA}$-F^1, G$_{PNA}$C$_{PNA}$-F^2, G$_{PNA}$C$_{PNA}$-F^3, G$_{PNA}$C$_{PNA}$-Cl^1, G$_{PNA}$C$_{PNA}$-Cl^2, G$_{PNA}$C$_{PNA}$-Cl^3, G$_{PNA}$C$_{PNA}$-Br^1, G$_{PNA}$C$_{PNA}$-Br^2 and G$_{PNA}$C$_{PNA}$-Br^3
whereas the isodensity surface value was fixed at 0.004 electrons/bohr^3 obtained from optimized structures at B3LYP/6-311++G** level of theory.

The interaction energy was calculated for all the considered systems using the counterpoise procedure $\left(\Delta E_{int}^{cp}\right)$, which was proposed by Boys and Bernardi (1970). It is defined as follows,

$$\Delta E_{int}^{cp} = E_{AB} - (E_A)_{\text{ in AB}} - (E_B)_{\text{ in AB}} \tag{1}$$

where E_{AB} is the total energy of the base pair, $(E_A)_{\text{ in AB}}$ represents the energy of nucleoside1 in the base pair (with the orbitals of nucleoside2 superimposed), and $(E_B)_{\text{ in AB}}$ represents the energy of nucleoside 2 in the base pair (with the orbitals of nucleoside1 superimposed)

2.1.1 Quantum molecular descriptors (QMD)

Studying the quantum molecular descriptors (QMD), including ionization potential (IP), electron affinity (EA), Chemical potential (μ), Chemical hardness (η), Chemical softness(S), Electrophilicity (ω), and Electronegativity (X) would provide an insightful understanding of the reactive sites of various molecular systems (Chattaraj et al. 2006; Padmanabhan et al. 2007; Uppuladinne et al. 2013; Jerbi and Springborg 2018). The QMD of all the considered systems were calculated based on Koopmans' theorem, which states that the negative energy of the highest occupied molecular orbital (HOMO) and lowest unoccupied molecular orbital (LUMO) is related to the IP and EA, respectively:

$$IP = -HOMO$$

$$EA = -LUMO$$

Additional descriptors: The formula for Electronegativity (χ), Chemical potential (μ), Chemical hardness (η), Chemical softness(S) and Electrophilicity (ω) by using the IP and EA, as shown below,

$$\text{Electronegativity } (\chi) = \frac{(IP+EA)}{2}$$

$$\text{Chemical potential } (\mu) = -\chi$$

$$\text{Chemical hardness } (\eta) = \frac{(IP-EA)}{2}$$

$$\text{Chemical softness}(S) = \frac{1}{\eta}$$

$$\text{Electrophilicity } (\omega) = \frac{\mu^2}{2\eta}$$

3 Results and discussion

Based on DFT calculations, the structural parameters, interaction energies and quantum molecular descriptors of all halogenated PNA base pair systems such as $G_{PNA}C_{PNA}$-F^1, $G_{PNA}C_{PNA}$-F^2, $G_{PNA}C_{PNA}$-F^3, $G_{PNA}C_{PNA}$-Cl^1, $G_{PNA}C_{PNA}$-Cl^2, $G_{PNA}C_{PNA}$-Cl^3, $G_{PNA}C_{PNA}$-Br^1, $G_{PNA}C_{PNA}$-Br^2 and $G_{PNA}C_{PNA}$-Br^3, were calculated at the B3LYP/6-311++G** level of theory and tabulated in Table 1 and 2.

3.1.1 Structural Parameters

The structural parameters such as bond distance of R─X, R─H and X/H•••Y (Å) and bond angle (º) (X=F, Cl and Br) for all optimized structures were measured and are shown in Table 1. The bond distances of R─X and R─H for all halogenated structures were found to be between ~1.332Å to 1.855Å and ~0.991Å to 1.040Å, respectively. The bond distance of X•••Y for all considered structures varied from ~1.762 to 5.253Å. Halogenation at position #2 affects the adjacent H-bond, causing N─H•••O stretching by about 4.449Å for Cl and 5.253Å for Br substitutions. Substituting the halogens at either #1 or #3 position leads to stronger nucleoside interactions than at position #2 in the base pair geometry. The bond distance X•••Y of halogenated PNA structures increases by about ~0.1Å to 0.4Å when compared to their natural counterparts, as by Parker et al. (2012). The bond angle R─X•••Y of $G_{PNA}C_{PNA}$-F^2, $G_{PNA}C_{PNA}$-Cl^1, $G_{PNA}C_{PNA}$-Cl^2, $G_{PNA}C_{PNA}$-Cl^3, $G_{PNA}C_{PNA}$-Br^1, $G_{PNA}C_{PNA}$-Br^2 and $G_{PNA}C_{PNA}$-Br^3 was found to be ~160º-172º, resulting in coplanar structures that are more favourable for the proper orientation of the σ-hole, as given in the ESP plot in Figure 2. The R─X•••Y of $G_{PNA}C_{PNA}$-F^1 and $G_{PNA}C_{PNA}$-F^3 were found to be ~70.8º and 48.7º, respectively, indicating that their planarity has been distorted due to the unequal charge distribution (Figure 2). The size of the halogen atom significantly affects the bond distances X/H•••Y by elongating about ~0.002Å to 3.294Å. The exhibited intra/inter-atomic R─X, R─H and also the X/H•••Y distances and bond angle R─X•••Y of Cl and Br substituted structures are found to be in the probable range for the formation of σ-hole, as per studies shown the stability of the halogen bond depends on proper orientation of the σ-hole which is associated with the covalent bonding region of R─X•••Y (Shields et al. 2010; Seidler et al. 2022; Smirnov et al. 2023).

3.1.2 Influence of halogenation on the interaction energy (E_{int})

The interaction energies (E_{int}) of all the halogenated PNA base pairs, including $G_{PNA}C_{PNA}$-F^1, $G_{PNA}C_{PNA}$-F^2, $G_{PNA}C_{PNA}$-F^3, $G_{PNA}C_{PNA}$-Cl^1, $G_{PNA}C_{PNA}$-Cl^2, $G_{PNA}C_{PNA}$-Cl^3, $G_{PNA}C_{PNA}$-Br^1, $G_{PNA}C_{PNA}$-Br^2 and $G_{PNA}C_{PNA}$-Br^3, were calculated at the B3LYP/6-311++G** level of theory and are evaluated with the available results (Table 1). The calculated E_{int} of all the halogenated PNA structures is tabulated concerning their substitutional positions (#1, #2, and #3), along with the results for halogenated DNA base pairs. The range of E_{int} for all halogenated PNA base pairs varies from -30.9kcal/mol to -6.9kcal/mol, whereas their respective H-bonded base pair has -29.53kcal/mol, as reported by Parker et al. (2012). The ascending order E_{int}, according to the position of halogen atom placed in considered systems, is as follows: $G_{PNA}C_{PNA}$-F^3 < $G_{PNA}C_{PNA}$-F^1< $G_{PNA}C_{PNA}$-Cl^1< $G_{PNA}C_{PNA}$-Br^1 <$G_{PNA}C_{PNA}$-Cl^3< $G_{PNA}C_{PNA}$-Br^3 < $G_{PNA}C_{PNA}$-Cl^2< $G_{PNA}C_{PNA}$-Br^2 < $G_{PNA}C_{PNA}$-F^2. It is noted that the E_{int} of $G_{PNA}C_{PNA}$-Br^1 and $G_{PNA}C_{PNA}$-Cl^3 were found to be almost similar at approximately 16.71kcal/mol and 16.31kcal/mol,

Table 1 Inter/Intra-nucleoside H/X bond distances (Å) R—X and R—H covalent bond length (Å), X/H•••Y bond distance (Å), R—X•••Y bond angles Θ (degrees) and interaction energies (E_{int}) for optimized halogenated PNA base pair geometries at B3LYP/6-311++G** level of theory

Base pair	bonds	R—X/Å	R—H/Å	X/H•••Y/Å	Θ/deg	E_{int} with PNA (in kcal/mol)	E_{int} with DNA (in kcal/mol) [$]
$G_{PNA}C_{PNA}$-F[1]	#1	1.382	-	2.978	70.8	-20.94	-
	#2	-	1.025	1.916	161.8		
	#3	-	1.017	2.132	164.9		
$G_{PNA}C_{PNA}$-F[2]	#1	-	0.994	4.135	169.5	-6.69	-
	#2	1.332	-	3.342	122.7		
	#3	-	1.000	2.654	112.0		
$G_{PNA}C_{PNA}$-F[3]	#1	-	1.033	1.762	175.7	-30.93	-
	#2	-	1.040	1.838	173.0		
	#3	1.383	-	1.789	48.7		
$G_{PNA}C_{PNA}$-Cl[1]	#1	1.723	-	2.627	165.4	-17.68	-18.72
	#2	-	1.017	2.663	164.4		
	#3	-	1.021	1.900	163.9		
$G_{PNA}C_{PNA}$-Cl[2]	#1	-	1.016	2.145	161.8	-11.83	-12.09
	#2	1.753	-	2.631	160.6		
	#3	-	1.008	4.449	160.4		
$G_{PNA}C_{PNA}$-Cl[3]	#1	-	1.024	1.834	171.9	-16.36	-16.68
	#2	-	1.022	2.615	163.1		
	#3	1.746	-	2.643	164.3		
$G_{PNA}C_{PNA}$-Br[1]	#1	1.830	-	2.937	156.6	-16.71	-24.16
	#2	-	1.000	2.914	163.8		
	#3	-	1.000	2.017	162.9		
$G_{PNA}C_{PNA}$-Br[2]	#1	-	0.998	2.321	161.3	-10.68	-18.02
	#2	1.855	-	3.010	150.7		
	#3	-	0.991	5.253	151.7		
$G_{PNA}C_{PNA}$-Br[3]	#1	-	1.001	1.980	171.8	-15.27	-20.39
	#2	-	1.000	2.869	161.8		
	#3	1.844	-	2.894	156.7		

$The interaction energy (Eint) values of halogenated GC base pair structures with plain forms obtained at B3LYP/6-31G* level of theory by J Parker et al.(2012).

respectively. The E_{int} of chlorinated structures, such as $G_{PNA}C_{PNA}$-Cl[1], $G_{PNA}C_{PNA}$-Cl[2], and $G_{PNA}C_{PNA}$-Cl[3] varies slightly from their respective natural counterparts, with values of -11.83kcal/mol, -16.36kcal/mol and -16.71kcal/mol showing a difference of approximately -0.24kcal/mol to -1.04kcal/mol. In the case of brominated structures such as $G_{PNA}C_{PNA}$-Br[1], $G_{PNA}C_{PNA}$-Br[2] and $G_{PNA}C_{PNA}$-Br[3], the E_{int} values were found to be -16.36 kcal/mol, -10.68 kcal/mol and -15.27 kcal/mol, while the E_{int} values for their respective natural counterparts as by Parker et al.(2012) were found to be -24.16 kcal/mol, -18.02kcal/mol and -20.39kcal/mol respectively. Among all the substitutional positions, it is evident from Table 1 that position #2 has the highest E_{int}, approximately -6.9kcal/mol, -11.83 kcal/mol, and -10.68kcal/mol for $G_{PNA}C_{PNA}$ with F, Cl and Br. Therefore, position #2 is the most favourable position for stronger interactions while stabilizing the adjacent bases to form higher-order strands.

3.1.3 Quantum molecular descriptors (QMD)

Based on Koopmans' theorem, we have calculated the QMD, including ionization potential (IP) and electron affinity (EA), Electronegativity (X), Chemical potential (μ), Chemical hardness (η), Chemical softness(S), and Electrophilicity (ω) for all the considered systems in the present work using the B3LYP/6-311++G** level of theory. The QMD of halogenated PNA structures are tabulated in Table 2 along with the non-halogenated PNA base pair results obtained B3LYP/6-31G*//B3LYP/6-311++G* level of theory (Indumathi et al. 2020). The IP of $G_{PNA}C_{PNA}$-F[1], $G_{PNA}C_{PNA}$-F[2], $G_{PNA}C_{PNA}$-F[3], $G_{PNA}C_{PNA}$-Cl[1], $G_{PNA}C_{PNA}$-Cl[2], $G_{PNA}C_{PNA}$-Cl[3], $G_{PNA}C_{PNA}$-Br[1], $G_{PNA}C_{PNA}$-Br[2] and $G_{PNA}C_{PNA}$-Br[3] ranges between ~5.66eV and 6.18eV whereas the non-halogenated $G_{PNA}C_{PNA}$ system is higher about ~7.32eV as by Indumathi et al. (2020). The Bar graph showing the calculated QMDs of all the halogenated PNA systems ($G_{PNA}C_{PNA}$-F[1], $G_{PNA}C_{PNA}$-F[2], $G_{PNA}C_{PNA}$-F[3], $G_{PNA}C_{PNA}$-Cl[1], $G_{PNA}C_{PNA}$-Cl[2],

Table 2 Reactivity descriptors: IP, EA, μ, η, ω, S and χ of halogenated PNA base pairs obtained at B3LYP/6-311++G** level of theory

Base pair	E_{HOMO} (in Hartrees)	E_{LUMO} (in Hartrees)	IP (in eV)	EA (in eV)	μ (in eV)	H (in eV)	ω (in eV)	S (in eV)	X (in eV)
$G_{PNA}C_{PNA}$-F[1]	-0.217	-0.085	5.90	2.31	-4.105	1.795	4.708	0.557	4.105
$G_{PNA}C_{PNA}$-F[2]	-0.219	-0.060	5.96	1.63	-3.795	2.165	3.347	0.462	3.795
$G_{PNA}C_{PNA}$-F[3]	-0.224	-0.070	6.10	1.90	-4.000	2.1	3.810	0.476	4.000
$G_{PNA}C_{PNA}$-Cl[1]	-0.208	-0.073	5.66	1.99	-3.825	1.835	3.973	0.545	3.825
$G_{PNA}C_{PNA}$-Cl[2]	-0.227	-0.054	6.18	1.47	-3.825	2.355	3.102	0.425	3.825
$G_{PNA}C_{PNA}$-Cl[3]	-0.228	-0.053	6.20	1.44	-3.820	2.38	3.075	0.420	3.820
$G_{PNA}C_{PNA}$-Br[1]	-0.210	-0.061	5.71	1.66	-3.685	2.025	3.347	0.494	3.685
$G_{PNA}C_{PNA}$-Br[2]	-0.227	-0.060	6.18	1.63	-3.905	2.275	3.347	0.440	3.905
$G_{PNA}C_{PNA}$-Br[3]	-0.224	-0.059	6.10	1.61	-3.855	2.245	3.293	0.445	3.855
[$]G_{PNA}C_{PNA}$	-	-	7.32	0.39	-3.849	3.471	2.134	0.288	3.849

[$]The compared reactivity descriptors values of GPNA-CPNA obtained at B3LYP/6-31G*//B3LYP/6-311++G** level of theory by Indumathi et al. (2020).

Figure 3 The IP, EA, μ, χ,η, S and ω in eVs plotted for $G_{PNA}C_{PNA}$-F[1], $G_{PNA}C_{PNA}$-F[2], $G_{PNA}C_{PNA}$-F[3], $G_{PNA}C_{PNA}$-Cl[1], $G_{PNA}C_{PNA}$-Cl[2], $G_{PNA}C_{PNA}$-Cl[3], $G_{PNA}C_{PNA}$-Br[1], $G_{PNA}C_{PNA}$-Br[2] and $G_{PNA}C_{PNA}$-Br[3] obtained at B3LYP/6-311++G** level of theory.

$G_{PNA}C_{PNA}-Cl^3$, $G_{PNA}C_{PNA}-Br^1$, $G_{PNA}C_{PNA}-Br^2$ and $G_{PNA}C_{PNA}-Br^3$) along with the non-halogenated $G_{PNA}-C_{PNA}$ system is given in Figure 3. The decrement in IP by about ~1.12eV to 1.66eV, indicating halogenated PNA structures required less energy for removing electrons than non-halogenated PNA systems. The halogenated systems' EA is about ~1.05eV to 1.92eV higher than the $G_{PNA}C_{PNA}$ system. While comparing EA among halogenated PNA systems, $G_{PNA}C_{PNA}-F^1$, $G_{PNA}C_{PNA}-F^3$ and $G_{PNA}C_{PNA}-Cl^1$ have the highest EA, about ~2.31eV, 1.90eV and 1.99eV, respectively. The chemical potential (μ) of #1 and #3 of fluorinated $G_{PNA}C_{PNA}$ and #2 and #3 of Brominated $G_{PNA}C_{PNA}$ are higher, about ~-0.006eV to -0.256eV, than others. Further, the increment of the ω value from about ~0.941eV to 2.674eV showed the ability of halogenated $G_{PNA}C_{PNA}$ systems reactivity has enhanced compared to the non-halogenated PNA base pair systems. In addition, the highest χ is observed for #1 and #3 of fluorinated $G_{PNA}C_{PNA}$, and #2 and #3 of Brominated $G_{PNA}C_{PNA}$ structures and were found to be ~4.110eV, 4eV, 3.864eV, and 3.918eV respectively. The remaining structures, such as $G_{PNA}C_{PNA}-F^2$, $G_{PNA}C_{PNA}-Cl^1$, $G_{PNA}C_{PNA}-Cl^2$, $G_{PNA}C_{PNA}-Cl^3$, and $G_{PNA}C_{PNA}-Br^1$ are found to be slightly lowered by about~0.012eV to 0.149eV, when compared to the non-halogenated $G_{PNA}C_{PNA}$ systems. Also, the η for halogenated $G_{PNA}C_{PNA}$ base pair is found to be lower, about ~1.016eV to 1.575eV, whereas the S of halogenated $G_{PNA}C_{PNA}$ base-pair structures are found to be higher, about ~0.132eV to 0.269eV than the non-halogenated $G_{PNA}C_{PNA}$ systems. From the results of QMD, a significant effect on $G_{PNA}C_{PNA}$ systems upon halogenations was observed in enhanced reactive properties by the increment of ω, χ, EA and S indicating their readiness towards the immediate chemical reactions.

Conclusion

The present work highlights the halogenation effect on $G_{PNA}C_{PNA}$ base pair systems concerning their positions by employing density functional theory (DFT). We found the size of the halogen atom affects the bond distance and the planarity of the base pairs based on the structural analysis. Additionally, we found that the Cl and Br substituted systems are most favourable for the spatial orientation of the σ-hole and maintaining good stability. However, we found that the quantum molecular descriptors that reveal the halogenated $G_{PNA}C_{PNA}$ systems are more susceptible to chemical reactions than their natural counterparts. Therefore, we concluded that halogenation in peptide nucleic acid systems significantly impacts both the structure and reactivity properties when compared to non-halogenated PNA. This study helps to understand the molecular characteristics of the halogenation effect on PNA base pair systems concerning substitutional position. Also, this study investigated how using various chemically modified PNA structures with halogenation could facilitate the progression of well-ordered triplexes for therapeutic applications. Our report on the structure and reactivity properties of halogenated PNA base pairs shows that it is worth understanding the physiochemical properties of such systems in therapeutic applications. Hence, our future study will explore the chemical properties, especially in the biological environment, by applying molecular dynamics simulation and experimental studies.

References

Álvarez-Martínez, F. J., Barrajón-Catalán, E., & Micol, V. (2020). Tackling Antibiotic Resistance with Compounds of Natural Origin: A Comprehensive Review. *Biomedicines*, *8*(10), 405. DOI: 10.3390/biomedicines8100405

Auffinger, P., Hays, F. A., Westhof, E., & Ho, P. S. (2004). Halogen bonds in biological molecules. *Proceedings of the National Academy of Sciences of the United States of America*, *101*(48), 16789–16794. https://doi.org/10.1073/pnas.0407607101

Benedetto Tiz, D., Bagnoli, L., Rosati, O., Marini, F., Sancineto, L., & Santi, C. (2022). New Halogen-Containing Drugs Approved by FDA in 2021: An Overview on Their Syntheses and Pharmaceutical Use. *Molecules*, *27*(5), 1643. DOI: 10.3390/molecules27051643

Boys, S.F., & Bernardi, F. (1970) The calculation of small molecular interactions by the differences of separate total energies. Some procedures with reduced errors. *Molecular Physics*, *19* (4), 553-566, DOI: 10.1080/00268977000101561

Chattaraj, P. K., Sarkar, U., & Roy, D. R. (2006). Electrophilicity Index. *Chemical Reviews*, *106*(6), 2065-2091. DOI: 10.1021/cr040109f

Danelius, E., Andersson, H., Jarvoll, P., Lood, K., Gräfenstein, J., & Erdélyi, M. (2017). Halogen Bonding: A Powerful Tool for Modulation of Peptide Conformation. *Biochemistry*, *56*(25), 3265-3272. DOI: 10.1021/acs.biochem.7b00429

Demidov, V. V., Potaman, V. N., Frank-Kamenetskil, M. D., Egholm, M., Buchard, O., Sönnichsen, S. H., & Nlelsen, P. E. (1994). Stability of peptide nucleic acids in human serum and cellular extracts. *Biochemical Pharmacology*, *48*(6), 1310-1313. https://doi.org/10.1016/0006-2952(94)90171-6

Dennington, R., Keith, T., & Millam, J. (2009). GaussView, Version 5.0.8.: Semichem Inc., Shawnee Mission KS

Fonseca Guerra, C., Bickelhaupt, F. M., Snijders, J. G., & Baerends, E. J. (2000). Hydrogen Bonding in DNA Base Pairs: Reconciliation of Theory and Experiment. *Journal of the American Chemical Society*, *122*(17), 4117-4128. DOI: 10.1021/ja993262d

Gaussian 09, Revision A. (2016). Gaussian, Inc., Wallingford, CT

Gomila, R. M., Frontera, A., & Bauzá, A. (2023). A Comprehensive Ab Initio Study of Halogenated A···U and G···C Base Pair Geometries and Energies. *International Journal of Molecular Sciences*, *24*(6), 5530. DOI: 10.3390/ijms24065530

Indumathi, K., Abiram, A., & Praveena, G. (2020). Effect of peptidic backbone on the nucleic acid dimeric strands. *Molecular Physics*, *118*(1), e1584682. DOI: 10.1080/00268976.2019.1584682

Inoue, M., Sumii, Y., & Shibata, N. (2020). Contribution of Organofluorine Compounds to Pharmaceuticals. *ACS Omega*, *5*(19), 10633-10640. DOI: 10.1021/acsomega.0c00830

Jerbi, J., & Springborg, M. (2018). Reactivity descriptors for DNA bases and the methylation of cytosine. *International Journal of Quantum Chemistry*, *118*(11), e25538. https://doi.org/10.1002/qua.25538

Kolář, M. H., & Tabarrini, O. (2017). Halogen Bonding in Nucleic Acid Complexes. *Journal of Medicinal Chemistry*, *60*(21), 8681-8690. DOI: 10.1021/acs.jmedchem.7b00329

Lee, C., Yang, W., & Parr, R. G. (1988). Development of the Colle-Salvetti correlation-energy formula into a functional of the electron density. *Physical Review B Condensed Matter*, *37*(2), 785-789. 10.1103/physrevb.37.785

Metrangolo, P., & Resnati, G. (2008). Chemistry. Halogen versus hydrogen. *Science*, *321*(5891), 918-919. DOI: 10.1126/science.1162215

Nielsen, P., Egholm, M., Berg, R., & Buchardt, O. (1992). Sequence-Selective Recognition of DNA by Strand Displacement with a Thymine-Substituted Polyamide. *Science* (New York, N.Y.), *254,* 1497-1500. DOI: 10.1126/science.1962210

Ochoa, S., & Milam, V. T. (2020). Modified Nucleic Acids: Expanding the Capabilities of Functional Oligonucleotides. *Molecules (Basel, Switzerland)*, *25*(20), 4659. https://doi.org/10.3390/molecules25204659

Padmanabhan, J., Parthasarathi, R., Elango, M., Subramanian, V., Krishnamoorthy, B. S., et al. (2007). Multiphilic Descriptor for Chemical Reactivity and Selectivity. *The Journal of Physical Chemistry A*, *111*(37), 9130-9138. DOI: 10.1021/jp0718909

Parker, A. J., Stewart, J., Donald, K. J., & Parish, C. A. (2012). Halogen Bonding in DNA Base Pairs. *Journal of the American Chemical Society*, *134*(11), 5165-5172. DOI: 10.1021/ja2105027

Patil, K. M., Toh, D. K., Yuan, Z., Meng, Z., Shu, Z., et al. (2018). Incorporating uracil and 5-halouracils into short peptide nucleic acids for enhanced recognition of A-U pairs in dsRNAs. *Nucleic Acids Research*, *46*(15), 7506-7521. DOI: 10.1093/nar/gky631

Seidler, M., Li, N. K., Luo, X., Xuan, S., Zuckermann, R. N., et al. (2022). Importance of the Positively Charged σ-Hole in Crystal Engineering of Halogenated Polypeptoids. *The Journal of Physical Chemistry B*, *126*(22), 4152-4159. DOI: 10.1021/acs.jpcb.2c01843

Shields, Z. P., Murray, J. S., & Politzer, P. (2010). Directional tendencies of halogen and hydrogen bonds. *International Journal of Quantum Chemistry*, *110*(15), 2823-2832. https://doi.org/10.1002/qua.22787

Smirnov, A. S., Mikherdov, A. S., Rozhkov, A. V., Gomila, R. M., Frontera, A., Kukushkin, V. Y., & Bokach, N. A. (2023). Halogen Bond-Involving Supramolecular Assembly Utilizing Carbon as a Nucleophilic Partner of I···C Non-Covalent Interaction. *Chemistry – An Asian Journal*, *18*(7), e202300037. https://doi.org/10.1002/asia.202300037

Uppuladinne, M. V. N., Jani, V., Sonavane, U. B., & Joshi, R. R. (2013). Quantum chemical studies of novel 2′-4′ conformationally restricted antisense monomers. *International Journal of Quantum Chemistry*, *113*(23), 2523-2533. https://doi.org/10.1002/qua.24492

Wang, C.R., & Lu, Q.B. (2010). Molecular Mechanism of the DNA Sequence Selectivity of 5-Halo-2′-Deoxyuridines as Potential Radiosensitizers. *Journal of the American Chemical Society*, *132*(42), 14710-14713. DOI: 10.1021/ja102883a

Yu, Y., Liu, A., Dhawan, G., Mei, H., Zhang, W., Izawa, K., Soloshonok, V. A., & Han, J. (2021). Fluorine-containing pharmaceuticals approved by the FDA in 2020: Synthesis and biological activity. *Chinese Chemical Letters*, *32*(11), 3342-3354. https://doi.org/10.1016/j.cclet.2021.05.042

Zdrowowicz, M., Wityk, P., Michalska, B., & Rak, J. (2016). 5-Bromo-2'-deoxycytidine — a Potential DNA Photosensitizer. *Organic and Biomolecular Chemistry*, *14,* 9312-9321. DOI: 10.1039/C6OB01446A